JOURNAL OF MATERIALS SCIENCE 19 (1984) 3626–3639

Oxide morphology and adhesive bonding on titanium surfaces

M. ASSEFPOUR-DEZFULY, C. VLACHOS, E. H. ANDREWS
Department of Materials, Queen Mary College, Mile End Road, London E1 4NS, UK

Titanium metal was subjected to two surface treatments (alkaline peroxide etch and chromic acid anodization) and resulting oxide morphology examined by high-resolution scanning electron microscopy in a Jeol 100-CX STEM. The effects of treatment time in alkaline peroxide upon oxide morphology were followed and parallel mechanical measurements made on the strengths of adhesive bonds between the metal and an epoxy resin. These strengths were measured after a standard environmental exposure, namely 120 h in water at 80° C. As time-of-treatment increases, a micro-porous oxide layer is developed and adhesive strength rises to a maximum. Prolonged treatment with alkaline peroxide produces a drastic fall in adhesive strength accompanied by gross etching of the metal surface without changes in the oxide morphology. The loss of adhesive durability in this case is therefore attributable to surface chemistry effects rather than morphological changes.

1. Introduction

The commercial use of surface pretreatments to improve the bondability of titanium and other metals is well established [1]. The first step is to employ mechanical abrasion and solvents to remove contaminants such as millscale, rolling lubricant and adventitious surface impurities. This should leave a clean, natural oxide surface. This oxide surface, however, does not afford optimum bond strength to structural adhesives, especially when the bond is exposed to moisture.

Significant improvements in bond durability in aqueous environments have been achieved using a variety of chemical and electro-chemical pretreatments, of which the most useful have been listed by Venables *et al.* [2]. Venables *et al.* proposed that the treatments could be divided into three categories as follows:

Group I, pretreatments which result in oxide layers with little or no micro-roughness (size scale $< 0.1\ \mu m$) or macro-roughness ($> 1\ \mu m$);

Group II, pretreatments which produce a large degree of macro-roughness;

Group III, pretreatments which produce a micro-porous oxide with little or no macro-roughness.

Venables and co-workers attribute the outstanding results from Group III pretreatments to the penetration of the micro-porous layer by the primer and/or liquid resin which, in turn, produces mechanical interlocking when the resin hardens [3, 4]. These authors do not, however, rule out the possibility that there are changes in the chemistry of the oxide layer which may contribute to enhanced bond durability.

So far we have mentioned three factors affecting bond durability, namely macro-roughness, oxide micro-morphology and oxide surface chemistry. One other factor that must obviously contribute is the mechanical or chemical stability of the oxide layer in the presence of heat and moisture. Thus Wegman and Bondnar [5] attributed the success of a modified phosphate fluoride pretreatment to the creation of a stable anatase TiO_2 surface in place of the original rutile form. However, Ditchek *et al.* [6] found that rutile oxide layers produced by chromic acid anodization (CAA) gave excellent durability in epoxy-to-metal bonds.

There is no doubt, however, that physical or chemical changes in the oxide layer do affect the integrity of adhesive bonds. For example, amorphous Al_2O_3 layers on Al alloys react almost instan-

0022–2461/84 $03.00 + .12

taneously with water to yield a "flakey" hydroxide [7] with small residual adhesive strength. Natan *et al.* [8] have also demonstrated the transformation of amorphous TiO_2 layers (of varying morphology and mode of creation) into a microcrystalline (anatase) form on exposure to 80° C water for periods exceeding one day. (These observations were made in the absence of an adhering resin, however.) In work reported elsewhere [9], we have observed both a decrease and a subsequent *increase* in the bond strength of titanium–epoxy joints with increasing time of exposure to 80° C water. (The increase was only observed at non-neutral environmental pH.) This is suggestive of slow chemical changes in the oxide layer.

To summarize, therefore, the features affecting bond strength and durability of adhesive joints between titanium (and its alloys) and structural adhesive resins (such as epoxy resins) appear to be as follows:

1. macro-roughness of surface;
2. micro-roughness or porosity of oxide layer. Oxide thickness may also play a part;
3. surface chemistry of oxide layer;
4. physical and chemical stability of oxide layer.

The research presented in this paper was carried out in an attempt to throw further light upon some of these effects. In particular we wished to define the macro- and micro-morphologies of titanium surfaces produced by the most effective surface pretreatments and to correlate the changes observed with measurements of the intrinsic adhesive failure energy θ_0 [10]. This parameter differs from the normal adhesive failure energy, θ, measured by fracture mechanics methods, in that it excludes the dissipative energy contribution to failure. Thus θ_0 represents the actual interfacial energy required to separate the adhering phase, and is a direct measure of inter-atomic bonding at the interface. This simple interpretation of θ_0 is, however, complicated if there is mechanical interlocking, as we shall see.

2. Materials and pretreatments

Commercially pure (99.4%) titanium, in the form of 1 mm thick sheet, was supplied by Titanium International Ltd. This metal is code-named Ti-2 and conforms to ASTM Gr-2. An elemental analysis gave the following results: 99.4% Ti, 0.03% N, 0.1% C, 0.01% H, 0.2% Fe, 0.25% O. The titanium was prepared for surface treatment by grinding on successive grades of (irrigated) silicon carbide paper, finishing with 800 grade, washed in acetone and dried in warm air.

TABLE I Detailed composition of alkaline peroxide etchants

Code	Weight of NaOH (g)	Volume of H_2O_2 (ml)
AP1	20	22.5
AP2	20	11.3
AP3	20	67.5

Plus de-ionized water to make 1 litre in all cases

Alkaline peroxide treatment was carried out using a solution typically comprising 20 g NaOH, 22.5 ml H_2O_2 and sufficient distilled water to give a final volume of 1 litre. Several different concentrations of the constituents were used for the adhesion studies as indicated in Table I. The metal was immersed in the solution at 70° C with agitation for the required etching time. On removal, the specimens were washed in distilled water and dried in warm air. Decomposition of the stock solution of H_2O_2 was monitored by titration against a standard solution of potassium permanganate.

Chromic acid anodization was effected at 23° C using an electrolyte consisting of 0.1 wt/wt solution of chromium trioxide (CrO_3) and 1 g litre^{-1} ammonium fluoride in distilled water. An aluminium cathode was placed 2.5 cm from the specimen (anode) and a voltage of 10 V applied for the required time of treatment. On removal, specimens were washed in distilled water and dried in warm air.

The epoxy resin employed was a diglycidyl ether of bisphenol A (Shell Epikote 828) with the stoichiometric ratio (2 : 5) of an amine hardener (Shell Epikure 114). Specimens were left to gel for 36 h at room temperature and postcured at 130° C for 1.5 h before being cooled slowly to ambient temperature at 0.5° C min^{-1}. The glass transition temperature of the cured resin was 73° C.

3. Experimental procedures

3.1. Mechanical testing

The adhesive failure energy, θ, was measured by the method of Andrews and Stevenson [9–11] which involves the pressurization of an enclosed circular flaw situated at the interface between the substrate and the resin. The specimen is shown in Fig. 1. The critical pressure, P_c, to cause specimen failure is measured and used to calculate failure

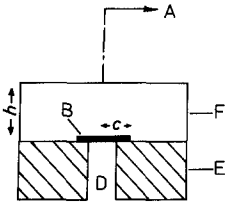

Figure 1 Specimen for the measurement of adhesive failure energy: (E) titanium block, (F) cast resin, (B) PTFE disc, (D) pressurization port, (A) circular symmetry about vertical axis.

energy from the formula [11],

$$\frac{P_c^2 c}{2E} = \theta f_2(h/c) \quad (1)$$

where c is the flaw radius, h is the resin thickness above the flaw, E is the Young's modulus of the resin, and

$$f_2(h/c) = \frac{1}{(1-\nu^2)}\left\{\frac{3}{32}\left[\left(\frac{c}{h}\right)^3 + \frac{c}{h}\frac{4}{1-\nu}\right] + \frac{2}{\pi}\right\}^{-1}, \quad (2)$$

where ν is the Poisson's ratio of the resin.

In these experiments we were concerned with the *durability* of the adhesive joints and bonded specimens of the kind shown in Fig. 1 were therefore immersed in water at 80° C and pH 7.8 for 120 h before drying, cooling to 23° C, and testing.

For the purpose of subsequent analysis it was necessary to measure not only the failure energy but also the crack velocity on failure. This was achieved by high speed photography using a "Hispeed" rotating prism camera (by John Hadland P.I. Ltd) in the streak mode. The method has been described previously [9] and details will not be repeated here.

3.2. Scanning electron microscopy

Small samples of the titanium were cut measuring 12 mm x 4 mm x 1 mm, one major surface being the treated surface. Care must be exercised not to damage the oxide layer on the treated surface by any kind of mechanical contact. The surface of interest was sputter-coated using a platinum target in a "Nanotech Semprep 2" sputter coating unit. To avoid obscuring the detail to be observed, the coating was kept at the minimum thickness (about 2 nm) necessary to suppress charging of the specimen in the microscope.

Specimens were examined in a Jeol 100-CX STEM operating at 40 kV in the secondary emission scanning mode, and stereo pair micrographs of the surfaces were obtained using a 7° tilt.

To observe the oxide layers in a cross-section, specimens were bent sharply to fracture the brittle oxide and then examined in the scanning mode as before.

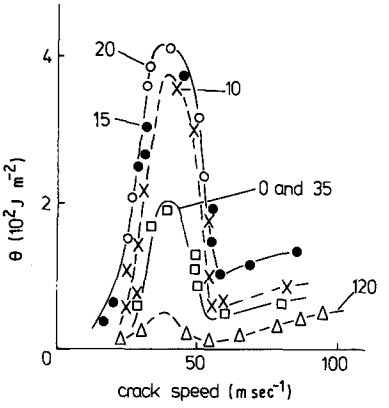

Figure 2 Adhesive failure energy, θ, as a function of crack velocity for epoxy resin bonded to titanium. Numbers indicate time of pre-treatment (min) in alkaline peroxide. Tests carried out after 120 h immersion in water at 80° C.

4. Results

4.1. Mechanical testing

Fig. 2 shows the variation of adhesive failure energy, θ, as a function of crack velocity for specimens of epoxy resin bonded to titanium. Five curves are shown, corresponding to different times of pretreatment in alkaline peroxide solution AP1 (see Table I), namely 10, 15, 20, 35 and 120 min treatment. As previously indicated, all tests were carried out after immesion of the specimen in water for 120 h at 80° C.

It is obvious from these data why it is necessary to measure crack velocity, since θ is strongly dependent on this variable. The complete plots of θ against $\dot{c}$, however, show unmistakably that θ depends upon the time of pretreatment. The peak in θ for untreated titanium is at approximately 200 J m^{-2} and this doubles to 400 J m^{-2} for 20 min pretreatment before falling away rapidly for longer pretreatment times.

These data can be further processed to provide the "intrinsic" adhesive failure energy, θ_0. This quantity is the energy required to break unit area of interfacial intermolecular bonds and is related to the measured failure energy, θ, by the following

equation, derived by generalized fracture mechanics theory [12].

$$\theta = \theta_0 \Phi(\dot{c}, T, \epsilon_0), \quad (3)$$

where Φ is a loss function for the resin dependent upon crack velocity ($\dot{c}$), temperature (T) and strain (ϵ_0). Taking logarithms,

$$\log \theta = \log \theta_0 + \log \Phi. \quad (4)$$

For specimens immersed at the same temperature and tested under the same conditions, Φ will be the same. Thus, assuming θ_0 is not a function of crack velocity

$$\log \theta_0 = \log \theta - \log \Phi$$
$$= \log \theta_{max} - \log \Phi_{max}.$$

The quantity $\log \Phi_{max}$ has been evaluated for the same resin under the identical conditions in previous papers [10, 13] and has the approximate value 2.4. It follows that a plot of $\log \theta_0$ against pretreatment time in AP1 solution is the same graph as that of $\log \theta_{max}$ against time except for an origin shift equal to -2.4. Thus the variation of θ_0 with pretreatment time is obtained and shown as Fig. 3. This diagram also includes data obtained using different concentrations of NaOH and H_2O_2 namely solutions AP2 and AP3. Within experimental error, no differences can be detected among the various solutions. Only one time-of-treatment was investigated from chromic acid anodization, namely 20 min. The value of θ_0 obtained for this system was 1.1 J m^{-2} compared with 0.75 J m^{-2} for untreated Ti (after the standard environmental exposure of 120 h at 80° C at pH 7.8).

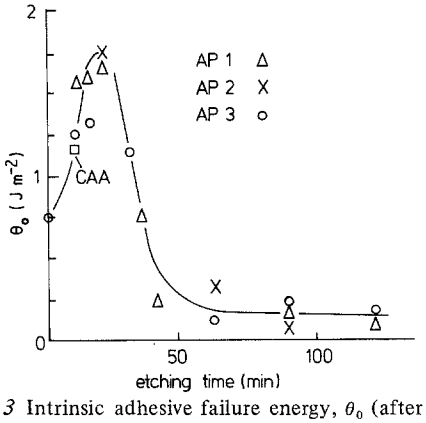

Figure 3 Intrinsic adhesive failure energy, θ_0 (after 120 h immersion at 180° C) as a function of time of pretreatment in alkaline peroxide for three different AP concentrations. One point refers to CAA treatment as indicated.

4.2. Oxide morphology from STEM-SEM

(Note: the stereo pairs referred to in this section may be viewed with a standard stereoscope with a 70 mm span between eyepiece centres and a 10 cm viewing distance.)

The original titanium surface, finished with 800 grade silicon carbon paper, is shown in Fig. 4 and reveals the expected grinding marks and embedded abrasive debris. At high magnification the oxide is seen to be smooth and continuous.

After 20 min pretreatment (Fig. 5) in AP1 solution, the grain structure is clearly visible as are a large number of elongated etch pits corresponding to either deformation twins induced by rolling and subsequent annealing, or to martensite platelets (an hexagonal phase of titanium) again produced by working. Both may be present.

At higher magnification (Fig. 6) the micro-morphology of the oxide surface is resolved and is seen to consist of a porous layer with a "cauliflower" texture and a rather "mountainous" topology. The scale of the texture or porosity is some 30 to 70 nm and the texture is uniform both inside and outside the etch pits.

Deformation of the specimen causes breaks in the oxide layer from which the oxide layer thickness can be inferred (Fig. 7). This thickness appears to be 50 to 100 nm.

After 1 h pretreatment in AP, grain boundaries are deeply etched as are the twinned regions. The micro-morphology of the oxide layer has not changed greatly (Fig. 8) although the "fingers" or "stalks" of oxide that constitute its fine texture are more discrete, the porosity is correspondingly

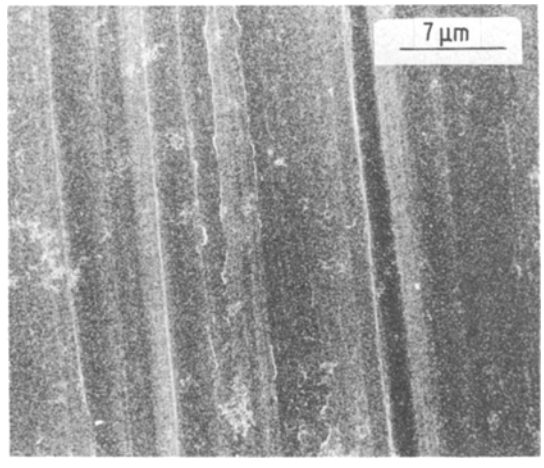

Figure 4 As-received titanium ground on 800 grade silicon-carbide paper.

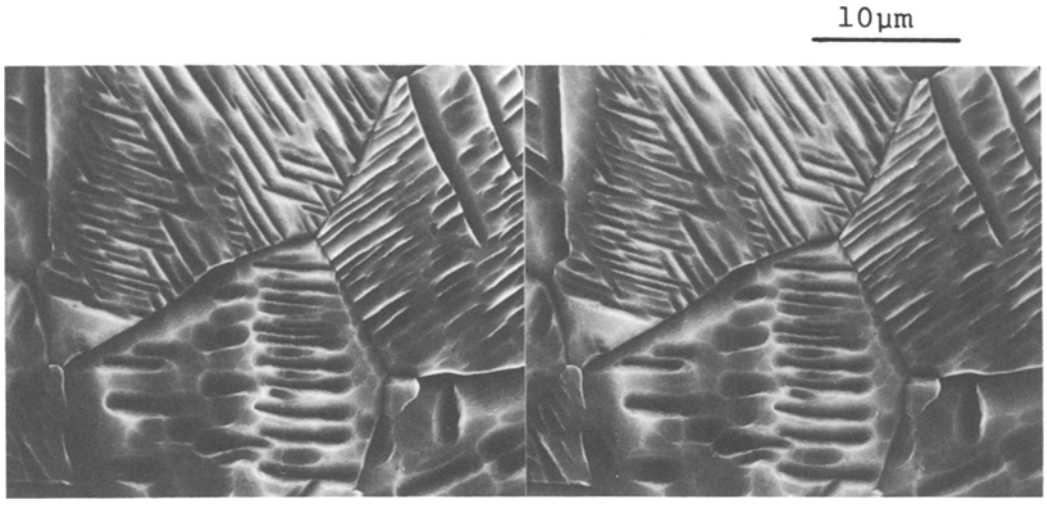

Figure 5 Titanium surface after 20 min treatment in alkaline peroxide, showing etching at grain boundaries and twins (or h c p martensite). Stereo pair.

greater and the scale of the texture has reduced to 15 to 30 nm. Deformed specimens show that the oxide layer thickness remains at about 50 to 100 nm. It is evident that gross etching and removal of surface material is occurring at a fairly constant oxide layer thickness (oxide is removed at the same rate at which it is formed).

After 2 h AP treatment, the oxide fine structure remains essentially the same, although marginally coarser than after 1 h. The oxide "stalks" are around 35 nm in diameter and very uniform (Fig. 9). Some care is required in attributing precise significance to the size scale of the fine structure and porosity, since this may vary from point to point on the same specimen.

The low magnification topology after 2 h in AP solution simply shows a continuation of the gross etching recognized after 1 h. Fig. 10 suggests that grain boundaries are so deeply etched and undercut that whole grains might be detachable from the surface.

We now turn to the surface morphology of specimens treated by chromic acid anodization (CAA). After 20 min treatment by CAA a uniform, porous structure has been established with pores of 35 to 70 nm diameter (Fig. 11). The structure

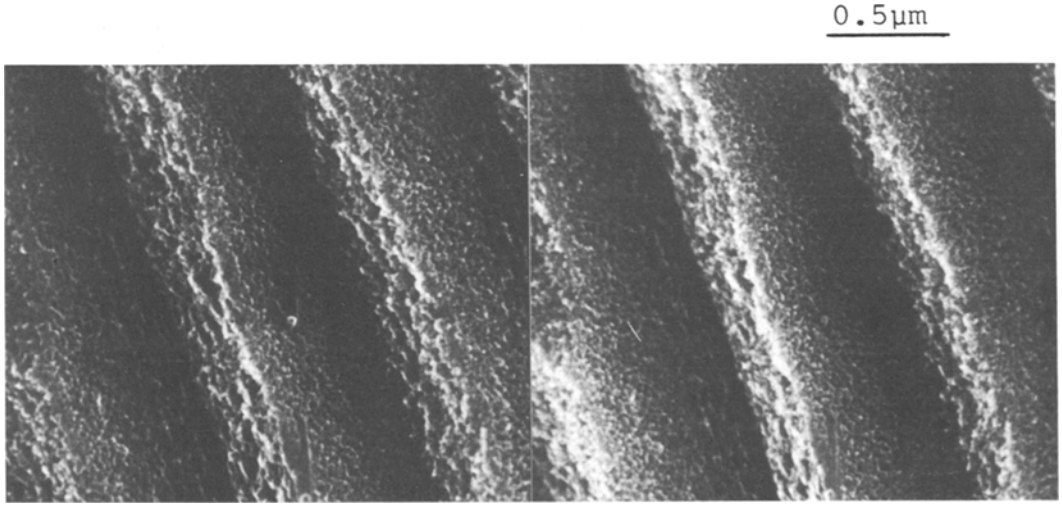

Figure 6 As Fig. 5 but at higher magnification showing porous oxide micromorphology. Stereo pair.

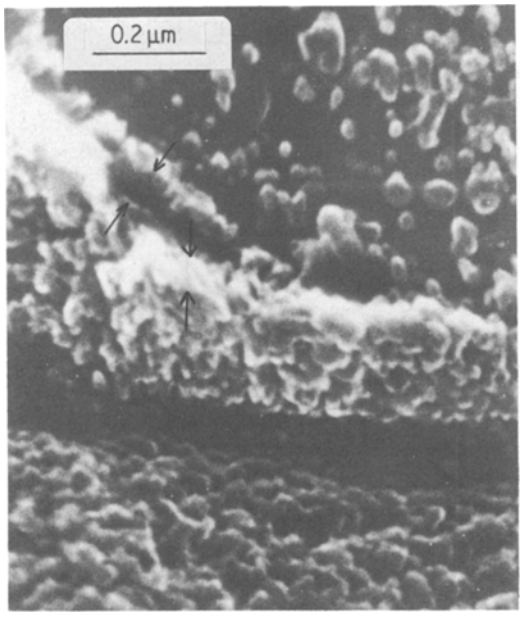

Figure 7 Titanium surface after 20 min AP treatment. Surface bent to fracture oxide layer.

consists of hollow, tubular oxide whiskers which are closely packed, often in such a way as to distort them from their circular form. There is no gross etching of the surface or grain boundaries with CAA treatment.

Bent specimens reveal that the oxide layer thickness after 20 min is some 300 nm (Fig. 12). The oxide layer breaks cleanly from the metallic substrate (unlike the layer produced by AP treatment) and "dimples" in the metallic substrate show clearly the site of oxide formation. Side-views of the oxide also exhibit an unexpected through-thickness periodicity of structure on the scale of 30 nm (Fig. 13).

A longer period (1.5 h) of CAA treatment produces no significant increase in oxide layer thickness. There is, however, evidence of disruption of the upper regions of the oxide layer visible in stereo micrographs (Fig. 14) and in side-views of the oxide layer (Fig. 13).

4.3. Hydration studies

The stability of the oxide layers in the presence of water was studied by immersing specimens in water for 100 h at 80° C and examining the resulting surfaces. Both tap water and distilled water were used.

Using tap water, the surfaces of both AP and CAA were found to be covered with small leaf-shaped crystals about 50 to 200 nm in size (Fig. 15). Similar crystals were found on untreated titanium surfaces but in much lower concentration. It is natural to suppose that these crystals are merely salts precipitated from solution since (as we shall see) they do not occur when distilled water is used. However, comparative studies on aluminium alloys (Fig. 16) show no signs of such crystals, the results of using tap water and distilled water being indistinguishable. Therefore, it seems that in the case of titanium there may be a chemical reaction between the dissolved calcium salts and the titanium oxide surface. We shall return to this point presently.

The results for distilled water treatment show

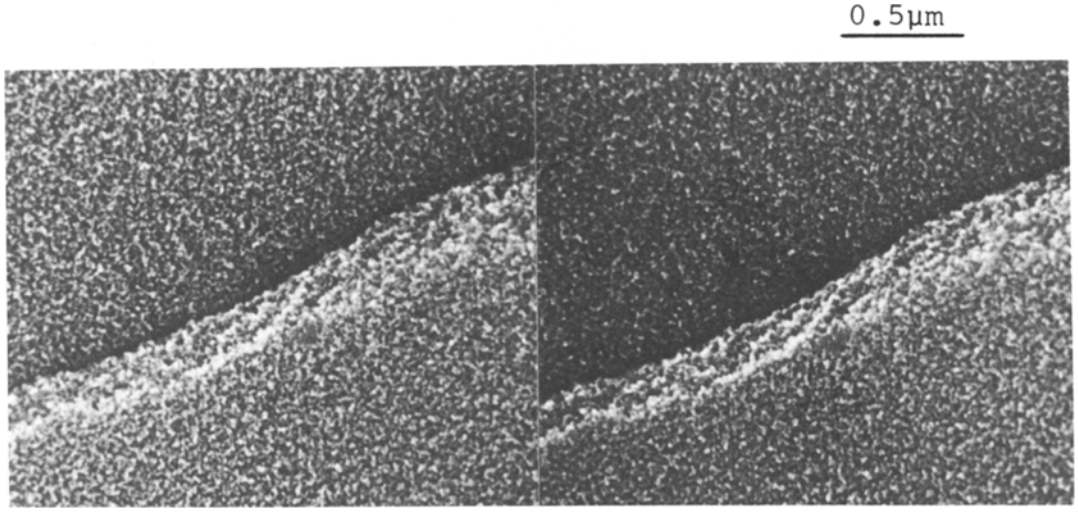

Figure 8 Titanium surface after 1 h AP treatment, showing oxide micro-morphology. Stereo pair.

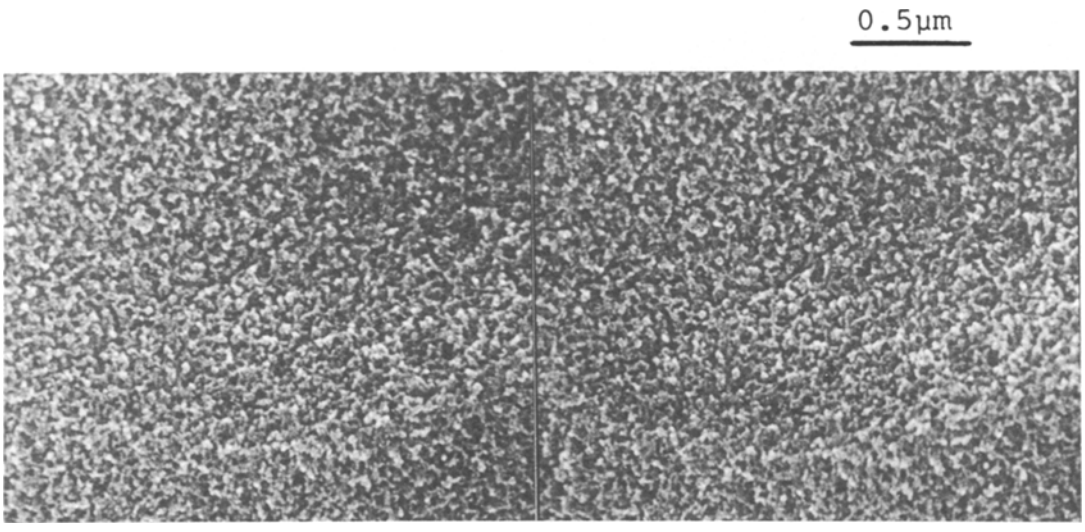

Figure 9 Titanium surface after 2 h AP treatment, showing oxide micro-morphology. Stereo pair.

no effect of water at low magnification. At high magnification, CAA treated specimens show some signs of attack. Such a surface is shown in Fig. 17 which should be compared with the unhydrated condition shown in Fig. 11. The porous tubular morphology is still evident, but patches of a continuous material have appeared and are beginning to obscure the tubular structure. Under stereo viewing it is evident that the tubular oxide has been deeply eroded and that the new phase may have a flake-like morphology similar to (though less dramatic than) that observed in aluminium alloys after a similar treatment (Fig. 16). The attack on titanium is obviously much slower than that on aluminium and its alloys.

Water-treated AP surfaces show little obvious change in structure, the porous "cauliflower" morphology being retained throughout. There is some evidence in stereo pairs that water treatment has produced surface erosion and increased porosity. It is also possible to find regions of the surface where a new continuous phase has begun to form, though such regions are not common.

For none of the prepared surfaces is the degree of water attack greater after 100 h at 80° C. If the surface is covered with resin and the resulting specimen immersed in water for 120 h at 80° C, the degree of interfacial attack must therefore be minimal as regards observable changes in the interfacial morphology.

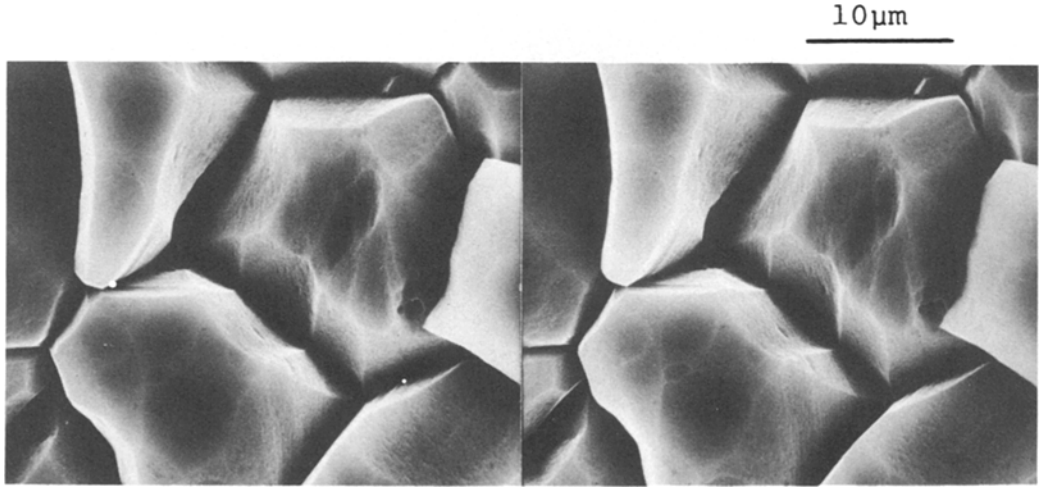

Figure 10 As Fig. 9 but at lower magnification. Stereo pair.

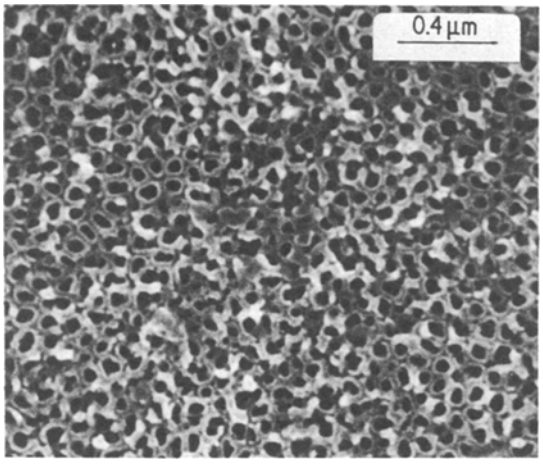

Figure 11 Titanium surface after 20 min chromic acid anodization. No surface etching observed.

The morphological effects of hydration on titanium oxide surface differ from those obtained by Natan *et al.* using a Ti–6Al–4V alloy [8]. For CAA treatment, their original morphology was identical to ours, but after as little as 25 h immersion at 85° C in distilled water, they obtained a crystal covered surface, identical in appearance to that which we obtained using tap water (Fig. 15). The crystals is question were identified by Natan *et al.* by small-angle diffraction as anatase. In NaCl solution at 140° C, they obtained a more flake-like anatase over-growth, but no visible attack below 100° C.

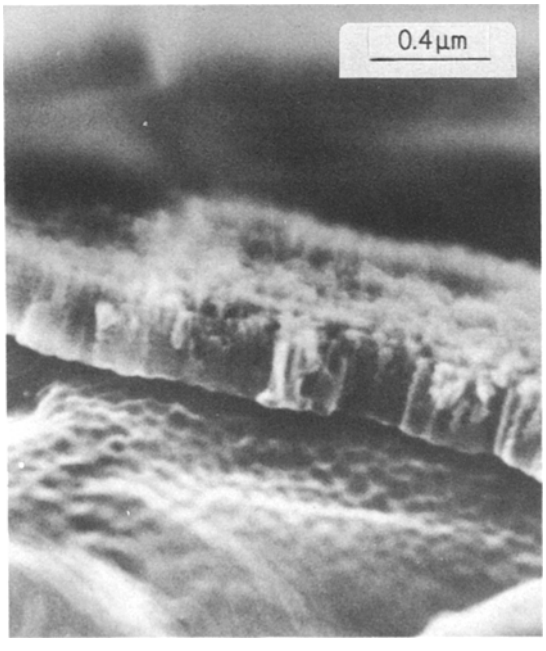

Figure 12 As Fig. 11 but surface bent to fracture oxide layer. Note dimples in metal surface below the oxide.

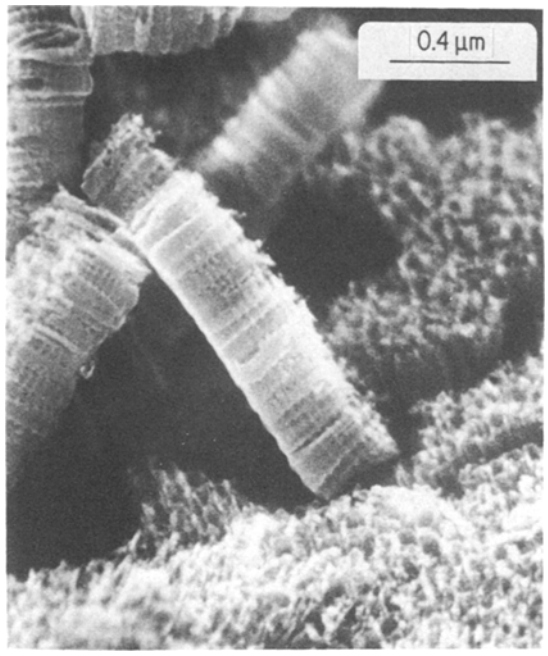

Figure 13 As Fig. 12 but after 1.5 h CAA treatment. Note vertical periodicity in oxide layer.

This rather confusing evidence suggests that both alloying ingredients (especially aluminium) and dissolved salts in the environmental aqueous phase, play an important role in determining the stability of the oxide in contact with water. Pure titanium in pure water appears to result in slow hydration compared with systems containing calcium and aluminium, although reaction may be accelerated by small temperature rises [14].

For AP treatments the story is identical. Natan *et al.* observed the growth of polygonal and elongated anatase crystallites over the whole surface, although the incubation period for nucleation of the new phase was longer than on CAA (and other) surfaces. This last observation does of course agree with our results in suggesting that the AP oxide is hydrolytically more stable than those produced by other surface treatments.

4.4. Fracture surface studies

The mechanical tests described earlier were carried out after immersion of specimens in tap, rather than distilled, water. It is therefore possible that anatase crystal formation is responsible for the observed deterioration of epoxy–titanium bonds

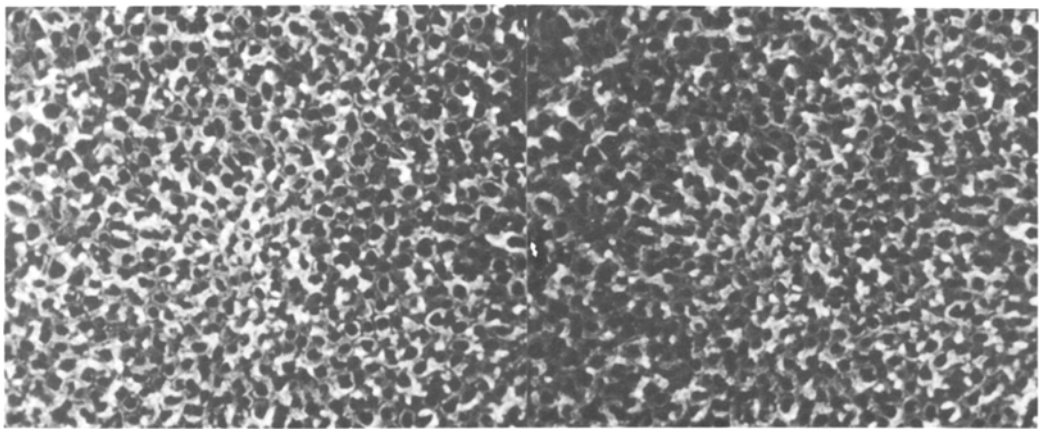

Figure 14 Titanium surface after 1.5 h CAA treatment. Stereo pair.

in water, corresponding to the effects shown in Fig. 15. In order to test this idea, further experiments were conducted in which surfaces were examined after epoxy resin had been cast on them, the specimens exposed to tap water for 120 h at 80° C, and the epoxy prised off again. To the eye, the resin appeared to separate cleanly from most of the surface and only such clear areas were examined in the STEM.

The surfaces obtained in this way gave very "noisy" images when sputter-coated to the thickness used on fresh surfaces. It was found necessary to double the coating time to 2 min in order to obtain clear images at × 50 000 magnification. (Note: coating times in excess of 1 min on clean surfaces produce aggregation of the Pt and spurious structures. The rule is always to use the minimum necessary to obtain noise-free imaging.)

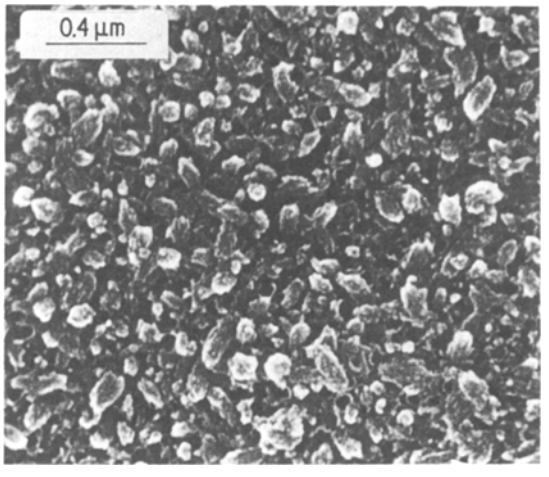

Figure 15 As Fig. 14 but immersed in tap water for 100 h at 80° C.

This imaging difficulty was *not* encountered with titanium surfaces prepared only by grinding and washing. The noise problem obviously indicates that epoxy resin has been retained by the treated surfaces in spite of their clean appearance. This is confirmed by closer examination.

Fig. 18 shows a 20 min CAA surface after epoxy separation. The tubular structure is still plainly visible beneath what appears to be an extremely thin, electron-transparent layer of resin. In places the surface structure appears with greater clarity and stereo-pairs show that such areas (marked A in Fig. 18) correspond to mounds which rise clear of the contamination layer. While interpretation needs to be done with caution it is obvious that the original tubular morphology is still present; that it nevertheless cannot be focused in the way that was possible originally or after direct water treatment; and that there must, therefore, be contamination of the surface with a non-conducting material resulting from the application, curing and removal of the epoxy resin. The nature of the retrained resin "layer" will be discussed in more detail later. What is clear, is that no anatase crystals are observed and the original tubular oxide morphology is un-affected even though the specimens were immersed in tap water.

AP treated surfaces also fail to reveal any anatase crystal formation. In the case of AP surfaces, there is the additional variable of AP treat-

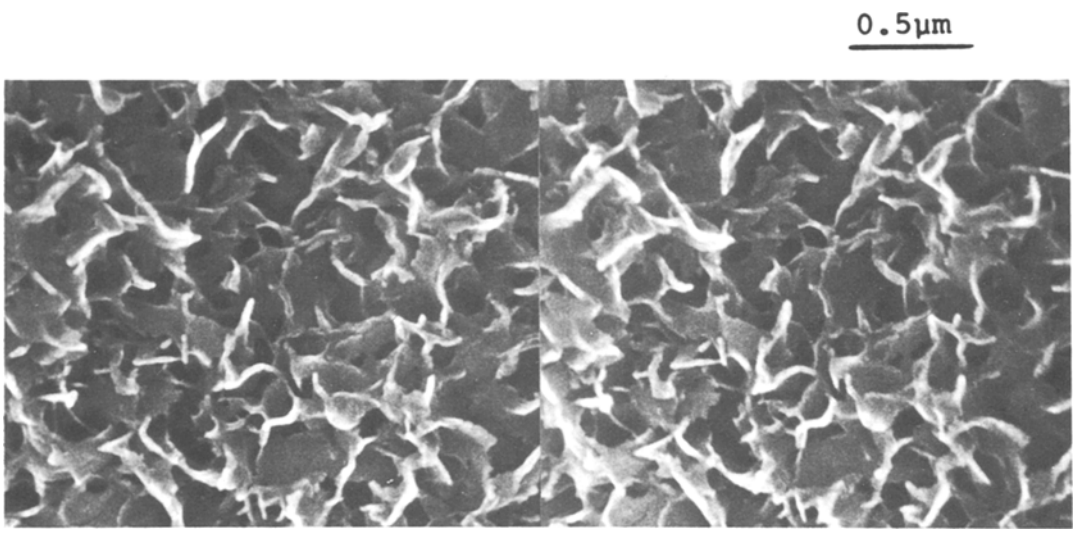

Figure 16 Aluminium, 4% magnesium alloy after CAA treatment and immersion in tap water for 100 h at 80° C. Stereo pair.

ment time which, it will be recalled, has a profound effect on durability (Fig. 3). Resin detachment experiments were performed on the 20 min treatment (which gave optimum mechanical durability) and on the 2 h treatment (for which the bond is less durable than untreated surfaces).

The surface of a 20 min AP specimen after epoxy removal is shown in Fig. 19 and shows extensive resin retention especially in the etched intra-granular grooves. The resin is easily distinguished in stereo micrographs from its "chunky" shape, but is also characterized by its glass like surface finish and by conchoidal fracture markings.

In contrast, on 2 h AP surfaces the epoxy breaks cleanly from the oxide except where it has penetrated deeply into etch pits and grain-boundary crevasses (see Fig. 20). That is, epoxy is only retained on 2 h AP surfaces where it is mechanically keyed, whereas it is retained adhesively over most of the 20 min AP surface.

At higher magnification, epoxy retention is evident even on the oxide plateaux for 20 min AP surfaces (Fig. 21), whereas flat areas of oxide are clean of resin in the 2 h AP specimens.

While mechanical keying, and consequent fracture through the resin, is evident in both cases,

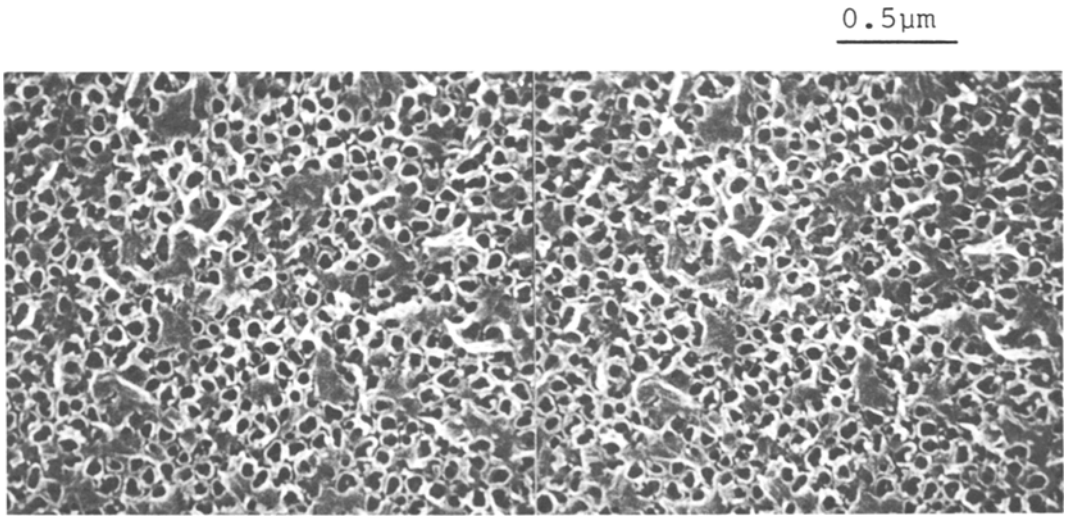

Figure 17 As Fig. 14 but immersed in distilled water for 100 h at 80° C. Stereo pair.

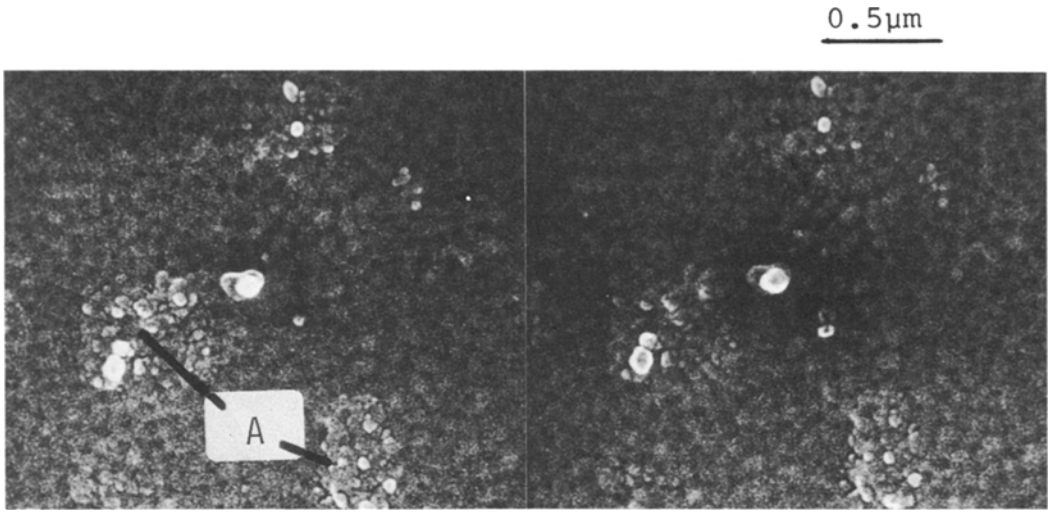

Figure 18 Fracture surface between titanium (20 min CAA) and epoxy resin after joint was immersed in tap water for 120 h and 80° C. Stereo pair.

therefore, it is clear that true adhesive bonding has been destroyed by water immersion in the 2 h AP specimens but not in the 20 min AP specimens. It is also clear that loss of adhesive strength in the 2 h AP specimens cannot be attributed to oxide hydration. This contrasts with the conclusions of Davis *et al.* [4] for aluminium alloys.

A final observation of interest is the formation in the resin of microbubbles of radius ~ 15 μm at the interface with the 2 h AP surfaces. These bubbles are identified by residual hemisphere of resin attached to the surface after removal of the epoxy coating (Fig. 22). The most obvious explanation is that resin, penetrating into the deep grain-boundary etch pits, displaces air which cannot rise through the viscous resin because of the small bubble size. No such bubbles are found on 20 min AP surfaces and their presence obviously contributes to water penetration and mechanical weakness in the over-etched specimens.

The results reported in this section therefore show that:

1. there is no evidence of hydration effects such as the formation of anatase crystals or hydroxide flakes at the epoxy–titanium interface after 120 h immersion at 80° C. We must look elsewhere for

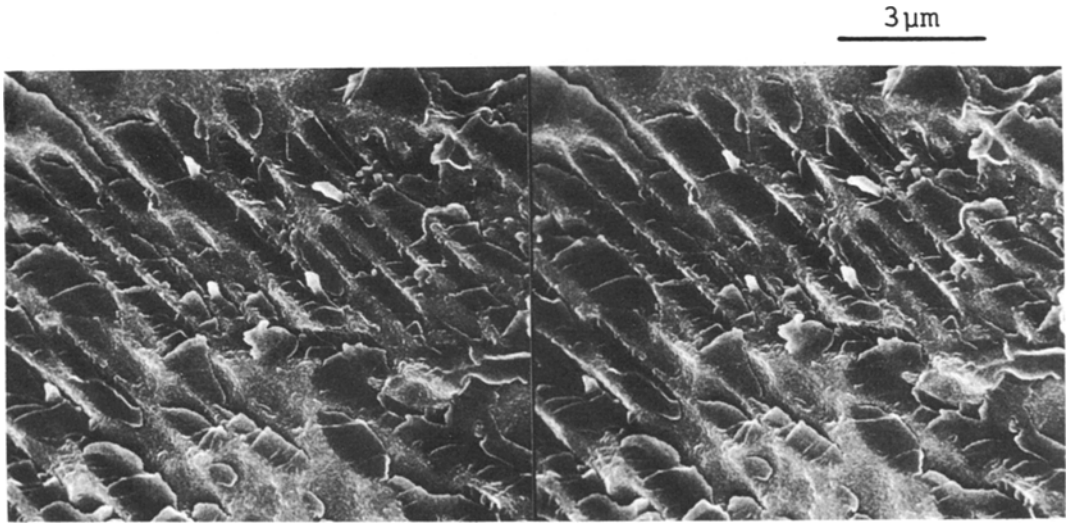

Figure 19 As Fig. 18 but titanium had been treated in AP for 20 min. Note adhering epoxy resin. Stereo pair.

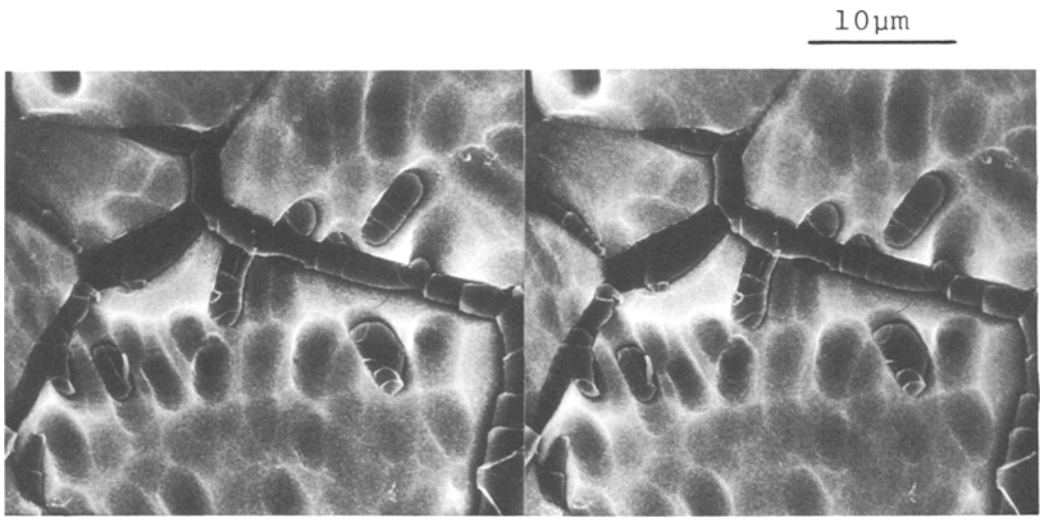

Figure 20 As Fig. 19 but AP treatment time was 2 h. Epoxy resin retained only in etch pits. Stereo pair.

an explanation of mechanical bond deterioration produced on this immersion time-scale;

2. resin is more readily displaced from the AP oxide surfaces than from the CAA surfaces. This may be due to the greater pore size of the tubular oxide structure in CAA and also to the uniform distribution of pores. It may also be due to chemical differences. On CAA surfaces, fracture seems to occur through the resin adjacent to the surface;

3. on AP surfaces there are always *some* regions where the epoxy breaks cleanly from the oxide. At the optimum (20 min) treatment time, however, there is much more retained epoxy than on over-etched (2 h) surface. On the latter the only retained resin is found in deep intergranular and intragranular etch pits where, presumably, it is mechanically keyed. Since the fine-scale oxide structure is similar at 20 min and 2 h AP treatment this suggests strongly that chemical differences exist between the two cases and that the different joint durabilities cannot be explained solely in terms of morphology;

4. bubbles of air trapped at the interface may contribute to joint weakness in over-etched AP specimens but this does not appear to be the major cause.

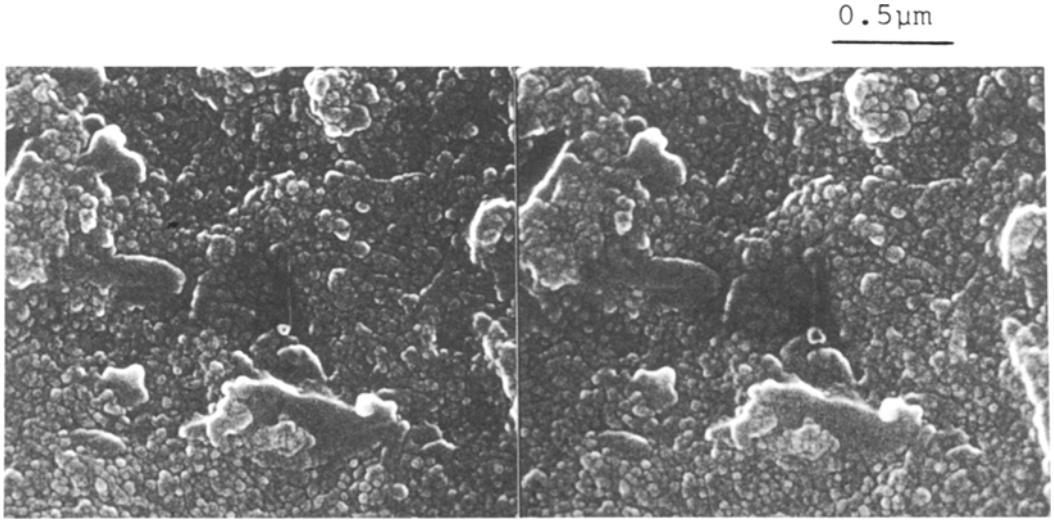

Figure 21 As Fig. 19 but at higher magnification. Note intimate attachment of smooth epoxy masses. Stereo pair.

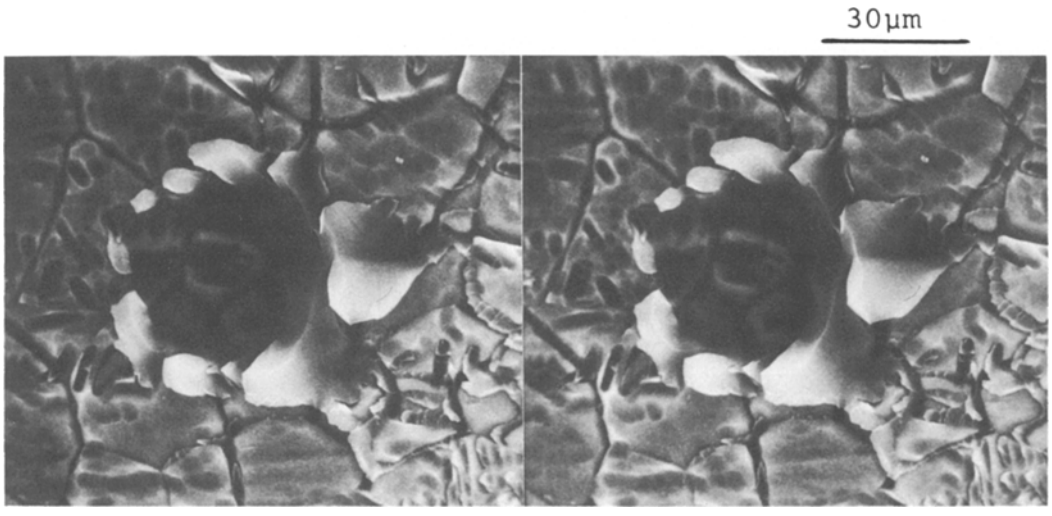

Figure 22 As Fig. 20 showing remains of air bubble. Stereo pair.

5. Discussion

Three basic explanations have been given for the improved durability achieved in adhesive joints by the pre-treatment of metal surfaces. These are:

1. mechanical inter-locking of the resin into a porous oxide layer;
2. improved interfacial bonding due to the interface chemistry, and
3. improved oxide stability in the presence of moisture.

The present work sheds light on all these proposed mechanisms in so far as they operate in the systems investigated.

Firstly, there is no doubt that the production of a porous oxide layer does coincide with a significant increase in the interfacial strength parameter, θ_0. It is also clear that, even after immersion in water for 120 h at 80° C, epoxy resin is retained after joint fracture on some of the porous oxide surfaces but not on untreated surfaces. Furthermore, penetration of the oxide microporosity by resin seems assured if only as a result of capillary forces. We thus arrive at the conclusion that a porous oxide provides a mechanical key for the resin and produces a composite interfacial region which will be difficult to break cleanly. This simply confirms the earlier conclusions of Venables *et al.* [3, 4]. Our evidence suggests that the regular tubular morphology produced by CAA treatment provides a better mechanical key than the less ordered porosity brought about by AP treatment.

It is much less clear, however, whether the morphological differences can account for the durability behaviour of the epoxy–titanium adhesion bond. Surfaces etched for different periods in AP solution exhibit a large difference in durability (i.e. in θ_0 values after 120 h at 80° C) without corresponding changes in micro-porosity. While gross etch pits occur after 1 to 2 h etching, these improve the mechanical keying and thus cannot be responsible for the observed deterioration in durability. High magnification micrographs show that resin separates cleanly from the microporous surface in over-etched specimens but is retained on a similar surface in optimally etched specimens. A chemical difference, therefore, seems to be indicated.

Chemical differences between oxides produced by different treatments seem indicated by the different rates of hydrolytic attack observed by Natan *et al.* in a Ti–6Al–4V alloy [8]. We also see such differences in commercially pure titanium.

This brings us to the third possible mechanism of bond deterioration in water, namely hydrolytically induced structural changes in the oxide. Our findings are quite definite here. For pure titanium in distilled water there is no significant attack after 100 h at 80° C, which seems to contrast with the results of Natan *et al.* on the titanium alloy and with our own results using tap water. Furthermore, when an epoxy covered surface is exposed to water for 120 h at 80° C, no morphological transformations in the oxide layer can be discerned even though joint strength has deteriorated severely. Of course, transformed

material may exist on a scale below the resolution of our micrograph. On balance, however, we conclude that for the system titanium–epoxy, the major strength loss on exposure to water occurs without transformation in the oxide layer.

The cause of θ_0 reduction, and thus of joint strength, on exposure to water thus appears to be the straightforward hydrolysis of the interfacial atomic bonds as was found previously for epoxy/glass joints [13]. Water diffusing through the epoxy reaches the interface and hydrolyses primary bonds formed between the epoxy network and the oxide layer during the curing reaction. The existence of such primary bonds is implied by earlier studies on the same titanium–epoxy system [10].

For CAA surfaces, true interfacial failure seems to occur only at isolated points, which may nucleate cracks when tested. The "interfacial" fracture which results appears to pass through the epoxy adjacent to the surface, but the retained layer of resin is sufficiently thin to be electron-transparent even after sputter-coating. It must also be remembered (a) that a transition from gross cohesive failure to apparent adhesive failure has already taken place as a result of water immersion; and that (b) the evidence for a retained epoxy "layer" is simply that the surface charges-up in the electron beam indicating the presence of non-conducting material. Taken together, these factors suggest that the fracture surface is not really cohesive through the resin, but that some organic material is retained on the oxide surface. This could consist of resin cores in the tubular pores or molecular fragments of the resin which are still firmly attached to the oxide surface. If these ideas are correct, we can still explain the effects of water exposure in terms of interfacial bond hydrolysis in spite of the retention of resinous material on the oxide after fracture.

In the case of AP treatments, hydrolytic deterioration of the interfacial bond is more complete after the standard exposure, some areas of all surfaces showing clean interfacial separation. The rate at which hydrolysis occurs varies with the time of treatment in AP solution and this suggests a variation in the density of primary interfacial bonds established on curing the resin, over-etched specimens having fewer such bonds. We cannot at present suggest the precise chemistry involved, but it may be associated with "poisoning" of the oxide by sodium from the etching solution.

Acknowledgement

This work was supported by a research grant from the Science and Engineering Research Council.

References

1. D. M. BREWIS (Ed.), "Surface analysis and pretreatment of plastics and metals" (Applied Science, Barking, 1982) Chs. 7 and 8.
2. J. D. VENABLES, B. M. DITCHEK and K. R. BREEN, Naval Air Systems Command, Washington D.C., Report AIR-52032-B (1980).
3. J. D. VENABLES, D. K. McNAMARA, J. M. CHEN and T. S. SUN, *Appl. Surf. Sci.* **3** (1979) 88.
4. G. D. DAVIS, T. S. SUN, J. S. AHEARN and J. D. VENABLES, *J. Mater. Sci.* **17** (1982) 1807.
5. R. F. WEGMAN and M. J. BONDNAR, *SAMPE Quart.* **5** (1973) 28.
6. B. M. DITCHEK, K. R. BREEN, T. S. SUN, J. D. VENABLES and S. R. BROWN, Proceedings 12th National SAMPE Technical Conference, Seattle, Washington, 1980 (Society for the Advancement of Material and Process Engineering, Azusa, CA, 1981) p. 882.
7. J. D. VENABLES, D. K. McNAMARA, J. M. CHEN, B. M. DITCHEK, T. I. MORGENTHALER, T. S. SUN and R. L. HOPPING, *ibid.*
8. M. NATAN, K. R. BREEN and J. D. VENABLES, Martin Marietta Laboratories Report MML TR 81-42(c) (1981).
9. C. VLACHOS, Ph.D. thesis, University of London (1982).
10. E. H. ANDREWS and A. STEVENSON, *J. Adhesion* **11** (1980) 17.
11. *Idem, J. Mater. Sci.* **13** (1978) 1960.
12. E. H. ANDREWS, *ibid.* **9** (1974) 887.
13. E. H. ANDREWS, HE PINGSHENG and C. VLACHOS, *Proc. Roy. Soc. (Lond.) A* **381** (1982) 345.
14. N. NATAN and J. D. VENABLES, *J. Adhesion* **15** (1983) 125.

Received 2 December 1983
and accepted 24 January 1984